High-Sensitivity Biosensor With Optical Tunneling Effect Excited by Long-Range Surface Plasmon Resonance

Zhuozhen Gao, Zheyu Hou, Pengyu Zhang, Xuanxiang Tong, Yanan Zhang, Zhibin Gan, Jian Shen, and Chaoyang Li

***Abstract*—Optical tunneling is an effect extremely sensitive to wavelength changes. In this article, we use this effect to design a new type of biosensor. The tunneling effect is excited by long range surface plasmon resonance, the energy is concentrated in the sensing medium in the form of standing waves, which lead a very high wavelength sensitivity and quality factor. By using COMSOL for finite element analysis, for the sensor structure of BK7/Cytop /Al_2O_3/Ag/Al_2O_3/sensing media/air, a quality factor of 10296 RIU^{-1} is achieved under angle modulation, a sensitivity of 170,000 nm/ RIU and a quality factor of 11333 RIU^{-1} are obtained under wavelength modulation. At the same time, the advantage of this structure is that there is no excessive requirement on the refractive index of the material, and a good sensing effect can be achieved even if the material is cheap and easy to prepare. After optimization, this structure is suitable for sensing media with a refractive index of 1.335-1.375, which can be applied to most liquid solutions.**

***Index Terms*—LRSPR, biosensor, optical tunneling, refractive index, standing wave.**

I. Introduction

OVER TIME, optical biosensors have become more and more attractive because they can detect biomolecules quickly and in real time without pre-labeling, which can be used in explosive environments, are resistant to electromagnetic interference, and have biocompatibility. The surface plasmon resonance (SPR) method is currently the dominant method in the field of optical biosensors [1]. However, the sensitivity of the traditional SPR sensor is relatively low, the full width at half maximum (FWHM) is large, and the penetration depth is shallow, which cannot meet the large analyte size [2], resulting in poor accuracy [3]. In order to improve the performance of the sensor and overcome these limitations, new SPR modes such as long-range surface plasmon resonance (LRSPR) [4], coupled plasma-waveguide resonance (CPWR) [5], and waveguide coupled SPR (WCSPR) [5] have been put forward. In the 1980s, the Sarid research team proved the excitation principle of LRSPR from theory and experiment [6]. Compared with other SPR modes, LRSPR has higher sensitivity, smaller FWHM and higher detection accuracy. In addition, metal thin film materials have more choices in the LRSPR sensing structure, not only using high reflection and low absorption metals (such as gold and silver) [7]but also use high absorption metals (such as Ni, Pd and V) [8], which expanded the application analysis of LRSPR technology in the chemical industry and other fields.

In recent years, the near-field optical method that uses the interface of two media to generate evanescent waves in the sub-wavelength region has attracted more and more attention. Optical tunneling is a special phenomenon that was first paid attention to by Newton. It refers to the ability of light waves (or photons) to pass through classically impenetrable material structures. This means that when the incident light propagates from the high refractive index medium layer to the low refractive index medium layer, and the incident angle is greater than the critical angle (total reflection angle), the light can enter the low refractive index medium layer due to the existence of the evanescent wave. If the thickness of the low refractive index medium layer is less than the penetration depth of the evanescent wave, the light can break through the limit of total reflection and continue to propagate forward. After passing into the next high-refractive-index medium layer, it will form transmission. The phenomenon of optical tunneling is also called Frustrated total-internal reflection (FTIR). In 1902, Elmer. E. Hall studied the FTIR phenomenon from both experimental and theoretical aspects. As the incident angle increases from the critical angle, the transmittance will increase sharply for s-polarized light. For p-polarized light, the transmittance is greater, and the transmittance will increase as the wavelength of the incident light changes [9]. In 1985, G. C. Bonazzola proposed that the maximum sensitivity mainly depends on the angle and polarization state of the incident light and the absorption characteristics of the third high-refractive-index dielectric layer [10]. In 2010, A. Q. Jian used the optical tunneling effect to be extremely sensitive to changes in refractive index to make refractometers [11]. The phenomenon of optical tunneling has a wide range of theoretical

Manuscript received September 29, 2021; revised October 30, 2021; accepted November 8, 2021. Date of publication November 12, 2021; date of current version December 20, 2021. This work was supported in part by the Finance Science and Technology Project of Hainan Province under Grant ZDKJ2020009, and in part by the Hainan Provincial Natural Science Foundation of China under Grant 2019RC054. *(Corresponding authors: Jian Shen; Chaoyang Li.)*

The authors are with the School of Information and Communication Engineering, Hainan University, Haikou 570228, China, and also with the State Key Laboratory of Marine Resource Utilization in South China Sea, Hainan University, Haikou 570228, China (e-mail: 20085400210124@hainanu.edu.cn; houzheyu@hainanu.edu.cn; pengyuzhang@hainanu.edu.cn; 20085400210165@hainanu.edn.cn; zhangyanan@hainanu.edu.cn; 20085400210122@hainanu.edu.cn; shenjian@hainanu.edu.cn; lichaoyang@hainanu.edu.cn).

Digital Object Identifier 10.1109/JPHOT.2021.3127569

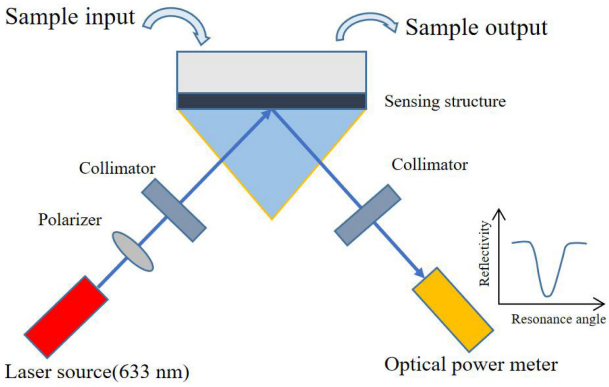

Fig. 1. Experimental schematic diagram based on prism structure.

and application values, and its discovery has also promoted the development of surface nonlinear optics.

In this paper, combining the principle of LRSPR and the tunneling effect caused by FTIR, a multilayer sensing structure with optical tunneling effect mediated by LRSPR is designed (prism/ Cytop/Al_2O_3/Ag/Al_2O_3/sensing medium/air). With the help of COMSOL, we tested the performance of the sensing structure under angle modulation and wavelength modulation through finite element analysis, at the same time, we verified its resonance curve characteristics and the range of maintaining high index characteristics through simulation calculations. Finally, the best matching film thickness of each layer structure and the change rule of resonance curve with various parameters are obtained.

II. Experimental Methods and Modeling Principles

A. Schematic Diagram of Sensor Based on Prism Structure

The schematic diagram of the sensor based on the prism structure is shown in the Fig. 1. The 633 nm laser source enters the prism at a certain angle of incidence after passing through the polarizer and collimator, then interacts with the sensing medium in the sensing structure, and finally reflects enter the power meter. We can draw the corresponding reflectivity curve by measuring the reflectivity, which reflects the liquid of different concentrations according to the resonance angle of the reflectivity curve.

B. Theoretical Description of Resonance Tunneling Phenomenon

As shown in Fig. 2, the refractive index of medium 1 and medium 3 is n_1, and the refractive index of medium 2 is n_2. The three interfaces are parallel to each other to form a structure with high/low/high refractive index. When the incident angle exceeds the critical angle of total reflection and when the thickness of the medium 2 is sufficiently thin, the evanescent field passing through the medium 2 into the medium 3 can be measured. This phenomenon is very similar to the tunneling effect of electrons passing through the barrier in quantum mechanics, which is called the optical tunneling effect. Because the transmitted and reflected fields are controlled by the distance between medium

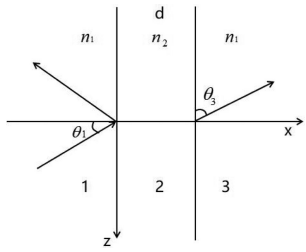

Fig. 2. Schematic diagram of optical tunneling.

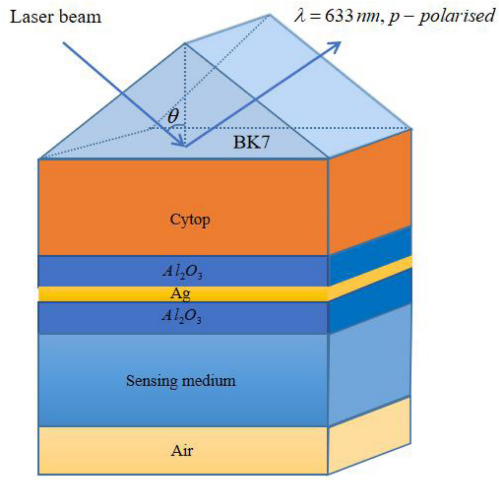

Fig. 3. Multilayer sensing structure.

1 and medium 3 during total reflection, people also call this phenomenon "frustrated total internal reflection". The optical tunneling effect can achieve very high transmission effects but it is different from the transmission of ordinary media [12].

Compared with the sensor constructed based on the SPR principle under wavelength modulation, optical tunneling can achieve higher sensitivity and resolution. The detection rate of the sensor can reach 85000 RIU^{-1}, and the resolution can reach 10^{-9}, higher than the traditional SPR refractometer out of four orders of magnitude[11]. Therefore, a sensor designed with tunneling effect may be able to achieve unprecedented sensitivity RI measurement.

C. Model Design

This paper designs the sensing structure shown in Fig. 3. The sensor consists of seven layers: prism (BK7), Cytop, Al_2O_3, Ag, Al_2O_3, sensing medium, and air.

The 633 nm light source enters the prism (BK7) through a polarizer (TM polarization). The refractive index of the BK7 is about $n_1 =$ 1.5151 at this wavelength. Among them, the Al_2O_3/Ag/ Al_2O_3 structure can be used as the excitation layer of LRSPR, and the thickness of Al_2O_3 is 150 nm. Cytop is a medium with a refractive index slightly higher than that of water. The refractive index is $n_2 =$ 1.337 [13] and the thickness is 800 nm. Its function is to match the refractive index of the object to be measured to achieve the effect of multiple total reflection. The initial refractive index of the sensing medium is $n_3 =$ 1.335, its

thickness is a fixed 2000 nm, above it is an infinite air medium, and the refractive index is n_4= 1.

Because the thickness of Al_2O_3 is 150nm, which is lower than the penetration depth of the evanescent wave. This sandwich structure produces suppressed total internal reflection while LRSPR occurs. Energy is not transmitted on the upper and lower surfaces of the metal like traditional LRSPR. Instead, a certain kind of transmission phenomenon occurs. The evanescent wave passes through the Al_2O_3 before it can be formed, and the total reflections occur when the Al_2O_3/sensing medium and the Al_2O_3/Cytop meet the total reflection condition. Finally, the two parts of energy generated by LRSPR are repeated multiple times after tunneling, then enter the sensing medium. By setting a reasonable thickness for Al_2O_3, the two parts of energy can be well coupled in the sensing medium. The energy entering the sensing medium is again reflected vertically on the air/sensing medium surface, and finally the energy stays in the sensing medium in the form of a standing wave.

Using matrix analysis method for the overall structure, for the enumeration of reflection of light from the prism an N-layer cast matrix system has been employed [14]. The thickness of each of the nanocomposite layers, T_k is considered along the z-axis. The RI and the permittivity of the k^{th} layers are represented by $n_k$and ε_k, respectively. The tangential components of the fields are continuous at the first edge to the last edge [15].

$$\begin{bmatrix} U_1 \\ V_1 \end{bmatrix} = M \begin{bmatrix} U_{N-1} \\ V_{N-1} \end{bmatrix} \tag{1}$$

where U_1 is the borderline items of the electric field and V_1 is the borderline items of the magnetic field at the periphery of the first layer in Eq. (1). Also, $U_{N-1}$and $V_{N-1}$are the respective fields at the periphery of the N^{th} layer. The characteristic matrix of the amalgamated sensor structure is denoted by M_{ij} and for transverse magnetically polarized light the characteristic matrix is expressed by the following Eqs. [16].

$$M_{ij} = \begin{pmatrix} \prod_{k=2}^{N-1} M_k \end{pmatrix}_{ij} = \begin{pmatrix} M_{11} & M_{12} \\ M_{21} & M_{22} \end{pmatrix} \tag{2}$$

With,

$$M_{ij} = \begin{pmatrix} \cos\beta_k & -(i\sin\beta_k)/q_k \\ -(iq_k\sin\beta_k) & \cos\beta_k \end{pmatrix} \tag{3}$$

Where,

$$q_k = \left(\frac{u_k}{\varepsilon_k}\right)^{1/2} \cos\theta_k = \frac{(\varepsilon_k - n_1^2 \sin^2\theta_1)^{1/2}}{\varepsilon_k} \tag{4}$$

And

$$\beta_k = \frac{2\pi}{\lambda} n_k \cos\theta_k (Z_K - Z_{K-1}) = \frac{2\pi T_k}{\lambda} (\varepsilon_k - n_1^2 \sin^2\theta_1)^{1/2} \tag{5}$$

After following some straightforward mathematical calculations, the following relationship of the reflection coefficient of reflected light for transverse magnetically polarized light can be derived as Eq. (6).

$$r_p = \frac{(M_{11} + M_{12}q_N)q_1 - (M_{21} + M_{22}q_N)}{(M_{11} + M_{12}q_N)q_1 + (M_{21} + M_{22}q_N)} \tag{6}$$

$$R_p = |r_p|^2 \tag{7}$$

The dispersion relation of the BK7 prism is given as follows. At this wavelength, use the following formula to calculate the refractive index of BK7 = 1.5151.

$$n_{BK7}(\lambda) = \sqrt{1 + \frac{m_1\lambda^2}{\lambda^2 - N_1} + \frac{m_2\lambda^2}{\lambda^2 - N_2} + \frac{m_3\lambda^2}{\lambda^2 - N_3}} \tag{8}$$

Among them, λ is the wavelength of incident light (633 nm), and m_1= 1.03961212, m_2= 0.231792344, m_3= 1.01046945, N_1= 0.00600069867, N_2= 0.0200179144, N_3= 103.560653.

Using the wavelength-dependent dispersion formula, the dispersion relationship of Al_2O_3 can be obtained as shown below,

$$n^2 - 1 = \frac{1.4313493\lambda^2}{\lambda^2 - 0.0726631^2} + \frac{0.65054713\lambda^2}{\lambda^2 - 0.1193242^2} + \frac{5.3414021\lambda^2}{\lambda^2 - 18.028251^2} \tag{9}$$

Where λ= 633 nm, the refractive index n= 1.7659 at this wavelength can be calculated.

According to the Drude-Lorentz model, the dispersion relation of silver can be obtained as shown below,

$$\varepsilon_{Ag}(\lambda) = 1 - \frac{\lambda^2\lambda_c}{\lambda_p^2(\lambda_c + i\lambda)} \tag{10}$$

among them λ_c= 1.761410×10^{-5} m , λ_p^2= 1.454110×10^{-7} m ,$\varepsilon_{Ag} = -17.81 + 0.067i$[17], [18].

D. Mathematical Modeling of Performance Parameters

In order to evaluate the performance of a model, we used the three parameters of sensitivity, full width at half maximum, and quality factor to test the performance under angle modulation and wavelength modulation respectively. Angle sensitivity($S_{\theta_{SPR}}$) is defined as the ratio of the shift of the SPR incident angle($\Delta\theta_{SPR}$) to the change of the refractive index(Δn_a) of the sensing medium. Wavelength sensitivity(S_λ)is defined as the ratio of the shift of the resonance wavelength($\Delta\lambda_{SPR}$) to the change of the refractive index of the sensing medium(Δn_a). The formula is expressed as follows,

$$S_{\theta_{SPR}} = \frac{\Delta\theta_{SPR}}{\Delta n_a} \tag{11}$$

$$S_\lambda = \frac{\Delta\lambda_{SPR}}{\Delta n_a} \tag{12}$$

The quality factor under sensor angle modulation depends on the sensitivity of the reflectance curve and the full width at half maximum, where $\Delta\theta_{0.5}$ is the spectral width of the reflectance curve corresponding to 50% reflectance, that is, the FWHM, which can be defined by the following equation:

$$FOM_\theta = \frac{S_{\theta_{SPR}}(^\circ/RIU)}{\Delta\theta_{0.5}}(RIU^{-1}) \tag{13}$$

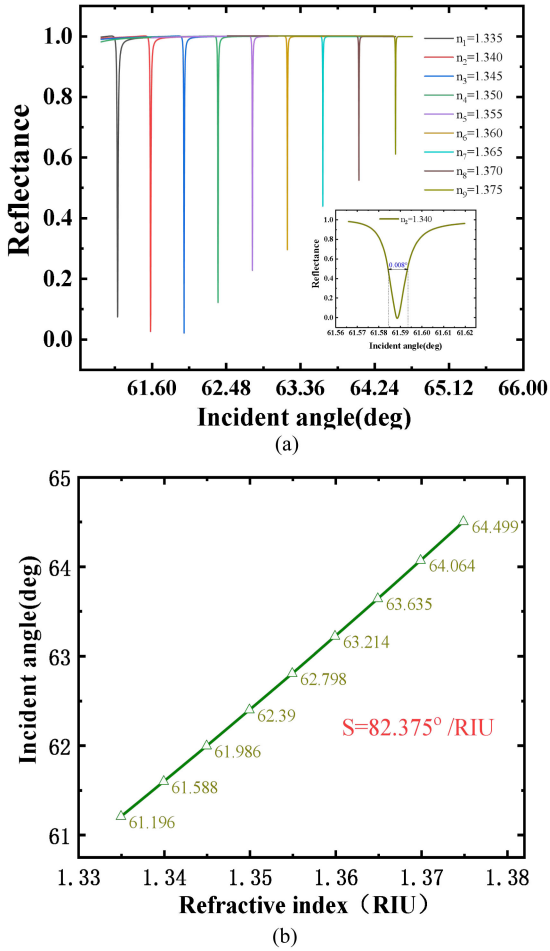

Fig. 4. (a) Reflectance curve under refractive index 1.335-1.375. (b) Sensitivity curve under refractive index 1.335-1.375.

The quality factor formula under wavelength modulation is described as

$$FOM_\lambda = \frac{S_\lambda(nm/RIU)}{\Delta\lambda_{0.5}}(RIU^{-1}) \tag{14}$$

Where $\Delta\lambda_{0.5}$ is the wavelength width corresponding to half of the reflectance curve of the reflectance curve [19].

III. Results and Discussion

A. Performance Under Angle Modulation

In the traditional LRSPR sensing experiment, the best resonance angle refers to the angle at which the coupled plasma wave energy is the largest, which is expressed on the reflectance curve as the corresponding angle at the lowest reflectance, while the resonance angle in this article refers to the best tunneling angle reached when the tunneling effect occurs and is also the angle corresponding to the lowest reflectivity. In order to study the performance of this model under angle modulation, under a light source with a wavelength of 633 nm, the refractive index range of the sensing medium is changed from 1.335-1.375, with 0.005 as the minimum unit, and the reflectance curve is shown in Fig. 4(a). We use COMSOL to establish

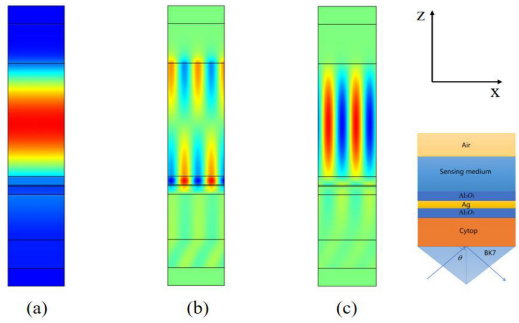

Fig. 5. The energy distribution of the structure designed by simulation (From bottom to top are perfect matching layer/prism BK7/Cytop/ Al_2O_3/Ag/ Al_2O_3 /sensing medium/air/perfect matching layer). (a) When the incident angle is 61.588 ° and the refractive index of the solution to be measured is 1.340, the energy distribution diagram in the structure. (b) When the resonance angle is reached at 61.588 °, the electric field component of Ex inside the structure. (c) The resonance angle is reached at 61.588 °, and the electric field diagram in the Hz direction inside the structure.

a two-dimensional rectangular model, as shown in Fig. 5, the rectangular width is 1000nm, the two sides are set as periodic boundary conditions, the upper and lower layers are perfectly matched layers, and the thickness is 316nm, from bottom to top are perfect matching layer/prism BK7/Cytop/Al_2O_3/Ag/ Al_2O_3/sensing medium/air/perfect matching layer. The number of grid cells is 7030, and the smallest mesh cell size is 0.101 nm.It can be seen that the reflectance curve in the refractive index range of 1.335-1.375 in the measurement range, the FWHM is very narrow, and the minimum reflectance is very low, which has a good sensing effect. When the refractive index $n_2 = 1.340$, its full width at half maximum is about 0.008°, and the lowest point of reflectance is 0.02. In addition, it can be seen from Fig. 4(a) that as the refractive index of the sensing medium increases, the reflectivity at the optimal resonance angle will also increase, which will not be conducive to the measurement in the actual engineering, and through simulation experiments, we think that it has good sensing properties in the refractive index range of 1.335-1.375, which is satisfactory for most solutions.

According to the reflectance curve shown in Fig. 4(a), the resonance angle and the corresponding refractive index are respectively taken as the x-axis and y-axis, and the average sensitivity of the designed structure can be calculated to be 82.375 °/RIU. The sensitivity linear curve is shown in Fig. 4(b). Therefore, it can be calculated that the quality factor realized by this structure is sensitivity/full width at half maximum, and the calculated quality factor is 10296 RIU^{-1}.According to current research, this quality factor is about 22 times the quality factor (466 RIU^{-1}) under traditional LRSPR angle modulation[20], and 1.76 times the angle sensitivity (46.6 °/RIU) under traditional LRSPR. The quality factor has reached about 423 times that of the traditional SPR angle modulation (24.3 RIU^{-1}). The relevant comparative data is in Table I. In Table II there are the performance parameters under different refractive index. This effect is a large improvement in the field of SPR biosensors.

Such a high quality factor is unexpected, so we need to explore the reasons for this situation. Fig. 5(a) shows the energy distribution inside the sensing model when the refractive index

TABLE I
COMPARISON OF PERFORMANCE PARAMETERS BETWEEN LRSPR+FTIR STRUCTURE AND LRSPR STRUCTURE UNDER ANGLE MODULATION

Type of structure	RI	Sensitivity	FWHM	FOM	Ref
BK7 prism/Cytop/Au/analyte	1.331–1.358	75.4 °/RIU	0.65°	116 RIU^{-1}	[21]
Prism/Au/fluoropolymer/Au/ diffraction grating/analyte	coli O157:H7	38 °/RIU	0.299°	127 RIU^{-1}	[22]
LaSFN9prism/Cytop/Teflon/ Poly(allylamine)/Au/analyte	1.331415-1.332570	46 °/RIU	0.1°	466RIU^{-1}	[20]
SF11prism/ppPFOE/Au/analyte	1.3525–1.3553	62.5 °/RIU	0.677°	92.3 RIU^{-1}	[23]
BK7prism/Cytop/ /Ag/ Al2O3 Al_2O_3/sensing media/air	1.335-1.375	82.375 °/RIU	0.008°	10296 RIU^{-1}	

TABLE II
SENSITIVITY AND FWHM AND FOM UNDER DIFFERENT REFRACTIVE INDEX

Refractive index	Sensitivity	FWHM	FOM
1.335	78.4°/RIU	0.015°	5226/RIU
1.340	79.6°/RIU	0.008°	9950/RIU
1.345	80.8°/RIU	0.007°	11542/RIU
1.350	81.6°/RIU	0.006°	13600/RIU
1.355	83.2°/RIU	0.0055°	15127/RIU
1.360	84.2°/RIU	0.004°	21050/RIU
1.365	85.8°/RIU	0.004°	21450/RIU
1.370	87.0°/RIU	0.0038°	22894/RIU
1.375	88.0°/RIU	0.0035°	25142/RIU

of the sensing medium is 1.340. When the resonance angle is 61.588°, the incident p-polarized light has an optical tunneling effect in the structure, and almost all the energy is confined in the water layer, and the tunneling energy ratio is close to 1.

As shown in Fig. 5(b) and (c), they are the x component of the electric field and the z component of the magnetic field, respectively. The z component of the magnetic field is the direction of energy propagation. There are two x components on the interface

TABLE III
COMPARISON OF PERFORMANCE PARAMETERS BETWEEN LRSPR+FTIR STRUCTURE AND LRSPR STRUCTURE UNDER WAVELENGTH MODULATION

Type of structure	RI	Sensitivity	FWHM	FOM	Ref
Fiber core/MgF2/Au/MgF2/analyte	1.33-1.38	5.276×10^3 nm/RIU	34 nm	156.19 RIU-1	[24]
SF14 prism/Teflon/Au/analyte	1.333–1.342	3.0×10^4 nm/RIU	-	-	[25]
BK7 prism/Teflon/Au/analyte	1.330-1.355	5.9×10^4 nm/ RIU	38 nm	1552 RIU^{-1}	[26]
BK7prism/Cytop/ Al_2O_3 /Ag/ Al_2O_3/ sensing media /air	1.3321-1.3328	1.7×10^5 nm/RIU	15 nm	11333 RIU^{-1}	

of the medium, which means that there are two modes of energy in the light wave tunneling process. In the principle of LRSPR generation, plasma waves are generated on the upper and lower surfaces of the metal medium. However, due to the occurrence of the tunneling effect, these two plasma waves are not coupled with each other, but produce tunneling in different directions, and finally couple into the sensing medium. In order to verify this hypothesis, we performed a parametric scan on the thickness of the Cytop. As shown in Fig. 6(a), the reflectance curve at a thickness of 200 nm-800 nm was drawn. The results show that when the thickness of the Cytop is 200 nm, the lowest point of reflectance exceeds 0.5. This means that more energy enters the prism, and when the thickness of the Cytop exceeds 400 nm, the lowest reflectance is about 0.2. According to the principle of total reflection, when the light wave enters the optically thin medium from the optically dense medium, the total reflection occurs. The evanescent wave will penetrate into the optically thin medium by a thickness of about half a wavelength, which is about 316 nm. Therefore, we can verify our hypothesis from Fig. 6(a) and (b). In Fig. 6(b), it is the local energy distribution map, and the total reflection phenomenon that occurs in the Al_2O_3/Cytop layer can be clearly seen. That is, part of the light wave is totally reflected at the lower Al_2O_3/Cytop interface. The latter light waves tunnel again into the sensing medium, and due to the presence of upper air, the light waves entering the sensing medium are reflected at the air/sensing medium, and the energy will stay in the sensing medium in the form of standing waves, this can be observed from the X component of the electric field in Fig. 5(b). The energy distribution in the sensing medium is 180° out of phase, which means the formation of a standing wave. The energy entering the sensing medium is caused by guiding the evanescent wave to produce suppressed total internal reflection. In the medium, a small change in the refractive index of the sensing medium will cause a large change in the resonance angle. This is also the reason why the model we designed has higher angular sensitivity than the traditional LRSPR structure. In order to obtain a reflectance curve with a higher penetration depth, we finally chose a Cytop with a thickness of 800 nm as the optimal thickness, actually, a thicker Cytop is also suitable,

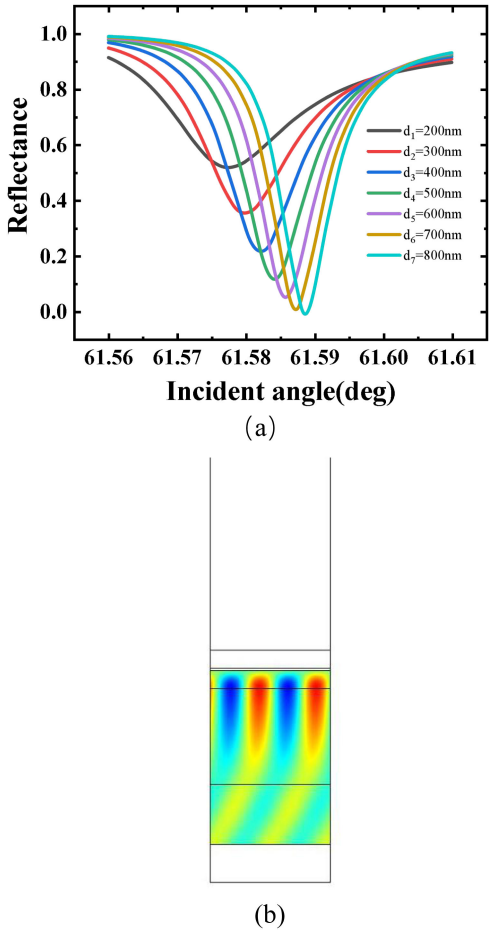

Fig. 6. (a) Reflectance curve under different thickness of Cytop. (b) The local energy distribution of the lower Al_2O_3/Cytop layer.

and at the same time, it can achieve close to 100% penetration of the sensing medium.

In order to verify the optical tunneling effect excited by LRSPR, we increased the thickness of Al_2O_3 from 150nm to 1000nm, and the z-direction distribution of the magnetic field is shown in Fig. 7(a). When the thickness of Al_2O_3 exceeds the propagation depth of the evanescent wave, the condition of suppressed total internal reflection is no longer satisfied. Al_2O_3/Ag/Al_2O_3 constitutes a separate model. When the incident angle meets the conditions of LRSPR, this high/low/high refractive index matching forms a larger energy barrier, and the energy produces something similar to quantum tunneling. Due to the matching of the refractive index of Cytop and the sensing medium, the total reflection effect occurs again at Al_2O_3/sensing medium and Al_2O_3/Cytop. The energy tunneling effect is finally transmitted to the sensing medium after it has occurred multiple times. For the specific study of the effect, please refer to the twelfth quotation [12]. The x-direction component of the electric field is shown in Fig. 7(b). In combination with Fig. 7(a) and (b), it can be observed that the LRSPR excited on the surface of the Ag film is no longer a simple evanescent wave which transports along the x direction, but produces a transmission in the z direction, forming a certain transmission effect. In this

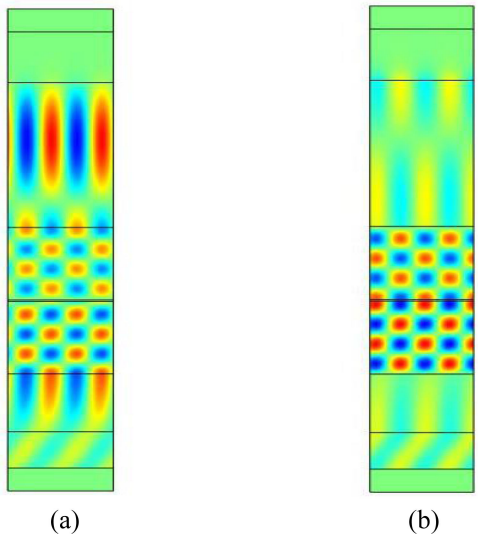

Fig. 7. (a) The Z-direction component of the magnetic field when the thickness of Al_2O_3 is 1000nm. (b) The x-direction component of the electric field when the thickness of Al_2O_3 is 1000nm.

article, we call it the optical tunneling effect. Therefore, we believe that this phenomenon similar to the optical tunneling effect is caused by LRSPR Inspiring, [12] our laboratory is still continuing to study this phenomenon.

B. Performance Under Wavelength Modulation

As the research on LRSPR becomes more and more in-depth, the sensitivity of LRSPR under angle modulation is relatively low. When using wavelength modulation, although the reflection peak produces a large wavelength shift, it is necessary to determine an accurate resonance angle. When the accuracy of the sensor is not high, it is difficult to accurately control the resonance angle every time, and a large error angle of incidence will cause the reflectivity to increase sharply, leading to large errors in the actual detection process.

In the actual measurement process of the sensor, sensitivity is more important for the evaluation of a model. Although the angle system in this model has a very high quality factor (10296 RIU^{-1}) and a very narrow full width at half maximum (0.008 °), the angle sensitivity S = 82.375 °/RIU, this sensitivity is improved compared to LRSPR, but compared with sensing SPR, the angular sensitivity is reduced. Compared with the SPR principle, the LRSPR principle has the advantages of deeper penetration depth and higher wavelength sensitivity. For this reason, we also tested the performance parameters of the model in this article under wavelength modulation.

As shown in Fig. 8, we tested the sensitivity under wavelength modulation within the range of the refractive index of the sensing medium from 1.3401 to 1.3408. By using COMSOL for parametric scanning, the incident angle was fixed at 61.588 °, and the wavelength was tested with 1nm as the minimum unit. The results show that when the refractive index changes from 1.3401-1.3402, the best resonance wavelength is shifted by 17 nm, the wavelength sensitivity is 170000 nm/RIU, and

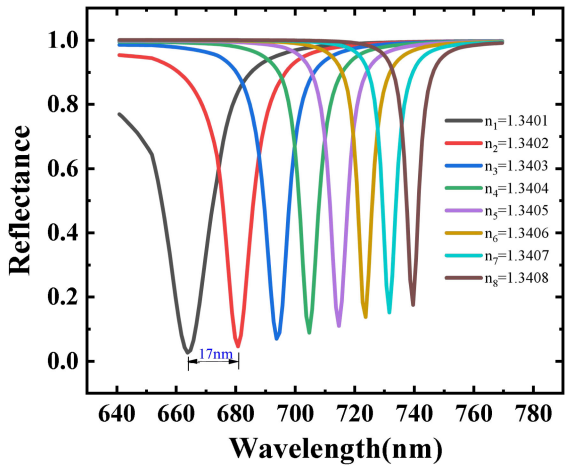

Fig. 8. Reflectance curve under wavelength modulation.

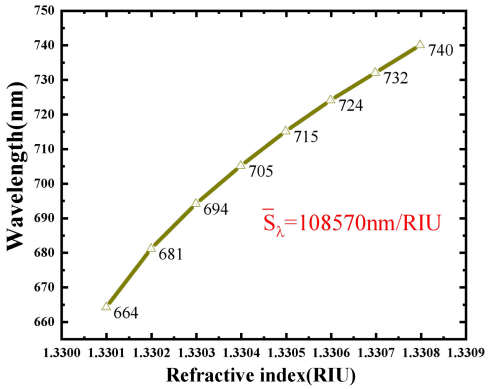

Fig. 9. Resonance wavelength when the refractive index is from 1.3301 to 1.3308.

the corresponding full width at half maximum is about 15 nm. The quality under wavelength modulation is 11333 RIU^{-1}. In addition, as shown in Fig. 9, we take the refractive index change as the X axis and the best resonance wavelength as the Y axis, and plotted 8 sets of data wavelength sensitivity curves, and obtained an average wavelength sensitivity of 108570 nm/RIU, according to the current research on SPR, the wavelength sensitivity comparison is shown in Table III.

IV. Discussion

The reason why this structure produces greater wavelength sensitivity is that resonant tunneling is very sensitive to changes in TM waves. The tunneling phenomenon mediated by LRSPR leads to multiple total reflections of light waves in the structure, which magnifies the difference of different wavelengths in the structure by multiples, so that even a very small refractive index change will cause a very large wavelength deviation. Due to the influence of the optical path difference, different wavelengths have different conditions for the generation of standing waves. Therefore, under the combined influence of the refractive index change and the optical path difference on the standing wave generation conditions, the wavelength change is very sensitive to small changes in the refractive index.

V. Conclusion

In this article, we designed a new type of biosensor which based on the optical tunneling effect. Due to LRSPR effect, the optical tunneling occurs between Al_2O_3 /Ag /Al_2O_3, which lead to multiple total reflection between Al_2O_3/Cytop and Al_2O_3/ sensing medium. Through this effect, we achieved high sensitivity under wavelength modulation, and very high quality factor under angle modulation. Through finite element analysis, under wavelength modulation, the highest sensitivity of 170000 nm/RIU, the average sensitivity of 108570 nm/RIU in the refractive index range of 1.3401-1.3408, and the highest quality factor of 11333 RIU^{-1} are achieved. Under angle modulation, a FWHM of 0.008°and a quality factor of up to 10296 RIU^{-1} are achieved. The sensitivity of the biosensor designed by the optical tunneling principle exceeds the sensitivity of the current SPR principle by 2 orders of magnitude, and the materials used are economical and easy to be obtained. We believe that this structure has potential applications in the field of biosensing.

Disclosures

The authors declare that there is no conflict of interests regarding the publication of this paper.

References

[1] P. Damborsky, J. Svitel, and J. Katrlik, "Optical biosensors," *Essays Biochem.*, vol. 60, no. 1, pp. 91–100, Jun. 2016.
[2] J. Dostálek, A. Kasry, and W. Knoll, "Long range surface plasmons for observation of biomolecular binding events at metallic surfaces," *Plasmonics,* vol. 2, no. 3, pp. 97–106, 2007.
[3] Y. Yuan and Y. Dai, "A revised LRSPR sensor with sharp reflection spectrum," *Sensors (Basel),* vol. 14, no. 9, pp. 16664–16671, Sep. 2014.
[4] P. Berini, "Long-range surface plasmon polaritons," *Adv. Opt. Photon.,* vol. 1, no. 3, pp. 484–588, 2009.
[5] F. C. Chien and S. J. Chen, "A sensitivity comparison of optical biosensors based on four different surface plasmon resonance modes," *Biosensors Bioelectron.*, vol. 20, no. 3, pp. 633–642, 2004.
[6] D. Sarid, "Long-range surface-plasma waves on very thin metal films," *Phys. Rev. Lett.*, vol. 48, no. 6, pp. 446–446, 1982.
[7] J. Hottin, E. Wijaya, L. Hay, S. Maricot, M. Bouazaoui, and J.-P. Vilcot, "Comparison of gold and silver/gold bimetallic surface for highly sensitive near-infrared SPR sensor at 1550 nm," *Plasmonics,* vol. 8, no. 2, pp. 619–624, 2012.
[8] P. Tobiška, O. Hugon, A. Trouillet, and H. Gagnaire, "An integrated optic hydrogen sensor based on SPR on palladium," *Sensors Actuators B: Chem.,* vol. 74, no. 1-3, pp. 168–172, 2001.
[9] E. E. Hall, "The penetration of totally reflected light into the rarer medium," *Phys. Rev. (Ser. I),* vol. 15, no. 2, pp. 73–106, 1902.
[10] G. C. Bonazzola, G. Ciocchetti, E. Conte, A. De Marco, M. Maringelli, and A. Trabucco, "Possible application of the optical tunnel effect to membrane biophysics," *Eur. Biophys. J.,* vol. 12, no. 1, pp. 51–55, 1985.
[11] A. Q. Jian, X. M. Zhang, W. M. Zhu, and M. Yu, "Optofluidic refractometer using resonant optical tunneling effect," *Biomicrofluidics*, vol. 4, no. 4, Dec. 2010, Art. no. 43008.
[12] S. Hayashi, H. Kurokawa, and H. Oga, "Observation of resonant photon tunneling in photonic double barrier structures," *Opt. Rev.,* vol. 6, no. 3, pp. 204–210, 1999.
[13] J.-Y. Jing, Q. Wang, W.-M. Zhao, and B.-T. Wang, "Long-range surface plasmon resonance and its sensing applications: A review," *Opt. Lasers Eng.,* vol. 112, pp. 103–118, 2019.
[14] A. Verma, A. Prakash, and R. Tripathi, "Performance analysis of graphene based surface plasmon resonance biosensors for detection of pseudomonas-like bacteria," *Opt. Quantum Electron.,* vol. 47, no. 5, pp. 1197–1205, 2014.

[15] J. B. Maurya, Y. K. Prajapati, V. Singh, J. P. Saini, and R. Tripathi, "Performance of graphene–MoS_2 based surface plasmon resonance sensor using silicon layer," *Opt. Quantum Electron.,* vol. 47, no. 11, pp. 3599–3611, 2015.

[16] M. S. Rahman, M. S. Anower, M. K. Rahman, M. R. Hasan, M. B. Hossain, and M. I. Haque, "Modeling of a highly sensitive MoS_2-graphene hybrid based fiber optic SPR biosensor for sensing DNA hybridization," *Optik,* vol. 140, pp. 989–997, 2017.

[17] A. K. Sharma and B. D. Gupta, "On the performance of different bimetallic combinations in surface plasmon resonance based fiber optic sensors," *J. Appl. Phys.,* vol. 101, no. 9, pp. 93–111, 2007.

[18] P. Zhang, T. Tang, J. Shen, L. Luo, C. Li, and J. Yao, "Spin hall effect of light in a prism-waveguide coupling structure with a magneto-optical bimetallic film," *Superlattices Microstructures,* vol. 128, pp. 136–143, 2019.

[19] M. S. Islam *et al.*, "Dual-polarized highly sensitive plasmonic sensor in the visible to near-IR spectrum," *Opt Exp.,* vol. 26, no. 23, pp. 30347–30361, Nov. 2018.

[20] R. Méjard, J. Dostálek, C.-J. Huang, H. Griesser, and B. Thierry, "Tuneable and robust long range surface plasmon resonance for biosensing applications," *Opt. Mater.,* vol. 35, no. 12, pp. 2507–2513, 2013.

[21] T. Kan, H. Kojo, E. Iwase, K. Matsumoto, and I. Shimoyama, "Long-range surface plasmon resonance sensor with liquid micro-channels to maintain the symmetry condition of the refractive index," *J. Micromechanics Microengineering,* vol. 20, no. 12, 2010, Art. no. 125005.

[22] Y. Wang, W. Knoll, and J. Dostalek, "Bacterial pathogen surface plasmon resonance biosensor advanced by long range surface plasmons and magnetic nanoparticle assays," *Anal. Chem.,* vol. 84, no. 19, pp. 8345–8350, Oct. 2012.

[23] L. Wang, X.-J. Liu, J. Hao, and L.-Q. Chu, "Long-range surface plasmon resonance sensors fabricated with plasma polymerized fluorocarbon thin films," *Sensors Actuators B: Chem.,* vol. 215, pp. 368–372, 2015.

[24] X. Feng *et al.*, "Long range surface plasmon resonance sensor based on side polished fiber with the buffer layer of magnesium fluoride," *Opt. Quantum Electron.,* vol. 49, no. 4, pp. 147–158, 2017.

[25] G. G. Nenninger, P. Tobiška, J. Homola, and S. S. Yee, "Long-range surface plasmons for high-resolution surface plasmon resonance sensors," *Sensors Actuators B: Chem.,* vol. 74, no. 1-3, pp. 145–151, 2001.

[26] M. Vala, S. Etheridge, J. A. Roach, and J. Homola, "Long-range surface plasmons for sensitive detection of bacterial analytes," *Sensors Actuators B: Chem.,* vol. 139, no. 1, pp. 59–63, 2009.